Reduction of Benzophenone and 9(10*H*)-Anthracenone with the Magnesium Complex [(2,6-*i*$Pr_2C_6H_3$-bian)$Mg(thf)_3$]

Igor L. Fedushkin,*[a] Alexandra A. Skatova,[a] Vladimir K. Cherkasov,[a] Valentina A. Chudakova,[a] Sebastian Dechert,[b] Markus Hummert,[b] and Herbert Schumann*[b]

Dedicated to Professor Helmut Schwarz on the occasion of his 60th birthday

Abstract: The reduction of benzophenone with the magnesium complex [(2,6-*i*$Pr_2C_6H_3$-bian)$Mg(thf)_3$] (**1**), containing the 1,2-bis[(2,6-diisopropylphenyl)imino]acenaphthene dianion, affords the pinacolato complex [(2,6-*i*$Pr_2C_6H_3$-bian)$Mg(thf)]_2[\mu$-$O_2C_2Ph_4]\cdot(C_6H_6)_4$ (**2**). The reaction of **1** with 9(10*H*)-anthracenone yields the 9-anthracenolato complex [(2,6-*i*$Pr_2C_6H_3$-bian)$Mg(OC_{14}H_9)(thf)_2$] (**3**). Complexes **2** and **3** were characterized by elemental analyses, UV/Vis, IR, and ESR spectroscopy, as well as by single crystal X-ray diffraction. Complex **2** dissociates in solution with splitting of the bridging pinacolato unit, forming the biradical diimino/ketyl complex [(2,6-*i*$Pr_2C_6H_3$-bian)$Mg(thf)(OCPh_2)$].

Keywords: ligand design · magnesium · radical ions · reduction

Introduction

Within the last decade, 1,2-bis[(2,6-diisopropylphenyl)imino]acenaphthene (2,6-*i*$Pr_2C_6H_3$-bian) became a very popular ligand in the coordination chemistry of transition metals.[1–6] The 2,6-*i*$Pr_2C_6H_3$-BIAN transition metal complexes turned out to be versatile reagents for a number of transformations of organic molecules, for example, for the catalytic hydrogenation of alkynes,[2] for C–C[3] and C–Sn[4] bond formations, and, particularly, for the catalytic olefin polymerization.[5] The rigidity and bulkiness of the ligand and its π-acceptor properties which cause an electron deficiency at the coordinated metal, render these complexes highly reactive towards organic substrates. We started our research on these complexes assuming that the 2,6-*i*$Pr_2C_6H_3$-BIAN ligand will accept up to four electrons (Scheme 1).

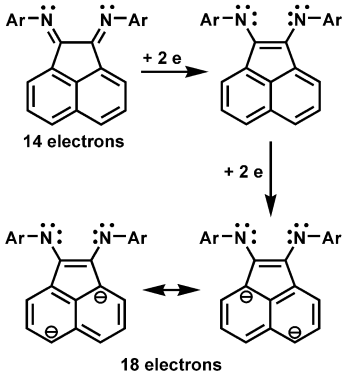

Scheme 1.

We could confirm this assumption by the isolation and structural characterization of the alkali metal derivatives of the mono-, di-, tri- and tetra-anions of the 2,6-*i*$Pr_2C_6H_3$-BIAN ligand.[7] We also succeeded in the isolation of monomeric 2,6-*i*$Pr_2C_6H_3$-BIAN complexes of magnesium and calcium[8] containing the 2,6-*i*$Pr_2C_6H_3$-BIAN dianion which were expected to be effective reducing agents. In this paper, we report on the products formed by the reduction of benzophenone and 9(10*H*)-anthracenone with [(2,6-*i*$Pr_2C_6H_3$-bian)$Mg(thf)_3$] (**1**).[8] It is known, that the reduction of aromatic ketones with one-electron reductants such as low-valent lanthanide[9] or titanium complexes[10] produces ketyl radicals, which, under certain conditions, form pinacol coupling products. On the other hand, very recently, it has been

[a] Prof. Dr. I. L. Fedushkin, Dr. A. A. Skatova, Prof. Dr. V. K. Cherkasov, Dr. V. A. Chudakova
G. A. Razuvaev Institute of Organometallic Chemistry of Russian Academy of Sciences
Tropinina 49, 603950 Nizhny Novgorod GSP-445 (Russia)
Fax: (+007) 8312-661-497
E-mail: igorfed@imoc.sinn.ru

[b] Prof. Dr. H. Schumann, Dr. S. Dechert, Dipl.-Chem. M. Hummert
Institut für Chemie der Technischen Universität Berlin
Strasse des 17. Juni 135, 10623 Berlin (Germany)
Fax: (+49) 30-3142-2168
E-mail: schumann@chem.tu-berlin.de

DOI: 10.1002/chem.200305235

reported, that Group 4 metal complexes[11] or lanthanide complexes[12] containing the dianionic 1,4-diaza-1,3-diene (DAD) ligand react with diphenylketone in the way of a 1,3-dipolar cycloaddition (Scheme 2).

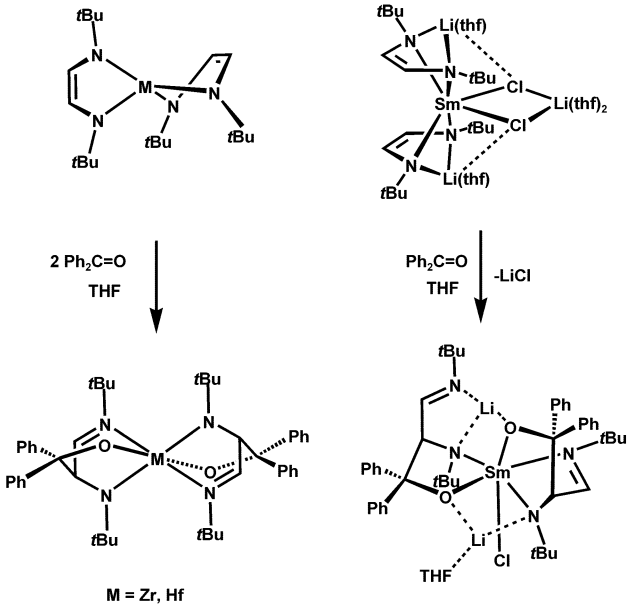

Scheme 2.

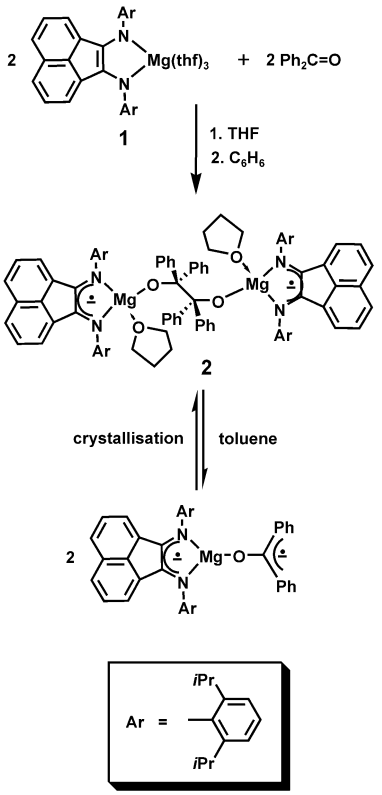

Scheme 3.

Results and Discussion

[{(2,6-*i*Pr$_2$C$_6$H$_3$-bian)Mg(thf)}$_2${μ-O$_2$C$_2$Ph$_4$}]·(C$_6$H$_6$)$_4$ (2): The addition of equimolar amounts of benzophenone to a THF solution of freshly prepared [(2,6-*i*Pr$_2$C$_6$H$_3$-bian)Mg(thf)$_3$] (**1**) causes an immediate change of the colour of the reaction mixture from green to red-violet. Evaporation of the solvent and crystallization of the crude product from benzene afforded deep red crystals of [{(2,6-*i*Pr$_2$C$_6$H$_3$-bian)Mg(thf)}$_2${μ-O$_2$C$_2$Ph$_4$}]·(C$_6$H$_6$)$_4$ (**2**) in a yield of 76% (Scheme 3). Compound **2** shows an ESR signal (single line, $g = 2.0042$) at room temperature, indicating the presence of ligand-centered radical anions. The magnetic moment of 2.57 BM calculated for the dinuclear complex differs only little from the value of 2.46 BM expected for a molecule with two unpaired electrons. According to this ESR spectroscopic result and to the result of the molecular structure determination of **2**, each of the two magnesium atoms is coordinated by a (2,6-*i*Pr$_2$C$_6$H$_3$-BIAN)$^{-\bullet}$ radical anion and the two magnesium atoms are bridged by a benzpinacolate group formed by dimerization of the benzophenone ketyl radical anions arising from the one-electron transfer from the dianionic (2,6-*i*Pr$_2$C$_6$H$_3$-BIAN)$^{2-}$ ligand in **1** to benzophenone.

[(2,6-*i*Pr$_2$C$_6$H$_3$-bian)Mg(OC$_{14}$H$_9$)(thf)$_2$] (3): [2,6-*i*Pr$_2$C$_6$H$_3$-bian)Mg(thf)$_3$] (**1**) reacts in situ with equimolar amounts of 9(10*H*)-anthracenone in THF at 50 °C within a few minutes. The reaction is connected with a change of the colour of the reaction solution from green to red. Removal of the solvent and crystallization of the remaining crude product from diethyl ether produces red crystals of [(2,6-*i*Pr$_2$C$_6$H$_3$-bian)-Mg(OC$_{14}$H$_9$)(thf)$_2$] (**3**) with a yield of 54% (Scheme 4). The complex is paramagnetic at room temperature corresponding to a magnetic moment of 1.87 BM, a value which is close to 1.73 BM expected for one unpaired electron per molecule. As confirmed by the molecular structure of **3** and its UV/Vis spectrum, the one-electron transfer from the

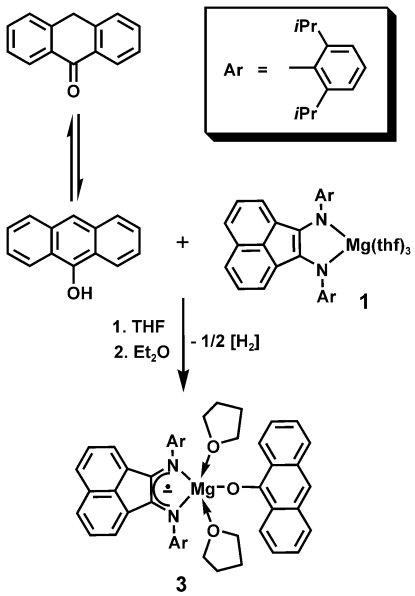

Scheme 4.

[2,6-*i*Pr$_2$C$_6$H$_3$-BIAN]$^{2-}$ dianion to the 9(10*H*)-anthracenone molecule does not lead to the formation of the respective ketyl radical anion, but causes deprotonation of the enolic tautomer 9-anthracenol yielding the 9-anthracenolate anion.

Molecular structures of 2 and 3: The molecular structures of **2** and **3** are depicted in Figures 1 and 2, respectively. The crystal data collections and structure refinement data of **2** and **3** are listed in Table 1, selected bond lengths and angles are listed in Table 2. In both complexes, the 2,6-*i*Pr$_2$C$_6$H$_3$-BIAN$^{-\bullet}$ radical anion acts as a rigid, chelating ligand.

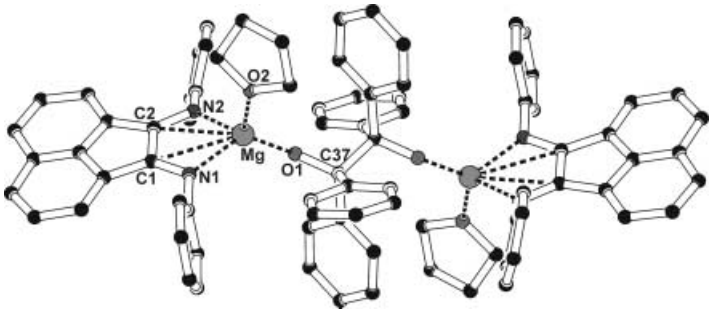

Figure 1. Molecular structure of **2**. The hydrogen atoms as well as the isopropyl groups at the N-phenyl substituents are omitted.

Table 1. Crystal data and structure refinement details for **2** and **3**.

Compound	**2**	**3**
empirical formula	$C_{106}H_{116}Mg_2N_4O_4{\cdot}4C_6H_6$	$C_{58}H_{65}MgN_2O_3$
F_w	1871.08	862.43
crystal system	monoclinic	triclinic
space group	$P2_1/c$ (no. 14)	$P\bar{1}$ (no. 2)
unit cell dimensions		
a [Å]	15.3287(2)	10.5809(3)
b [Å]	14.4373(1)	12.9119(3)
c [Å]	24.6010(3)	19.6879(2)
α [°]	90	97.951(2)
β [°]	98.336(1)	94.524(2)
γ [°]	90	113.139(1)
V [Å^3]	5386.81(10)	2423.24(9)
Z	2	2
ρ_{calcd} [g cm^{-3}]	1.154	1.182
μ [mm^{-1}]	0.079	0.083
F(000)	2008	926
crystal size [mm^3]	0.44×0.26×0.24	0.38×0.20×0.18
$\theta_{min}/\theta_{max}$ [°]	1.34/26.00	1.87/25.00
index ranges	$-18 \le h \le 18$	$-12 \le h \le 12$
	$-17 \le k \le 16$	$-13 \le k \le 15$
	$-21 \le l \le 30$	$-23 \le l \le 23$
refls collected	34797	14446
independent refls	10537	8298
R_{int}	0.0989	0.1259
refls with $I > 2\sigma(I)$	5703	2791
max/min transmission	0.9781/0.3904	0.9781/0.6111
data/restraints/parameters	10537/136/629	8298/0/585
GOF on F^2	1.031	0.915
final R indices [$I > 2\sigma(I)$]		
R_1	0.0849	0.0898
wR_2	0.2001	0.1288
R indices (all data)		
R_1	0.1579	0.2655
wR_2	0.2403	0.1730
largest diff. peak/hole [e A^{-3}]	0.645/−0.385	0.285/−0.310

Table 2. Selected bond lengths [Å] and angles [°] for **2** and **3**.[a]

Compound	**2**	**3**
	bond lengths	
Mg–O1	1.839(2)	1.889(4)
Mg–O2	2.035(3)	2.135(4)
Mg–O3		2.073(4)
Mg–N1	2.107(3)	2.113(5)
Mg–N2	2.079(3)	2.205(5)
N1–C1	1.324(4)	1.334(7)
N2–C2	1.331(4)	1.339(7)
N1–C13	1.440(4)	1.430(5)
N2–C25	1.435(4)	1.431(6)
C1–C2	1.457(5)	1.432(6)
O1–C37	1.397(4)	1.303(5)
C37–C37′	1.605(7)	
	bond angles	
O1-Mg-O2	116.65(12)	93.55(17)
O1-Mg-O3		101.03(17)
O2-Mg-O3		85.49(16)
O1-Mg-N1	128.10(12)	120.11(16)
O2-Mg-N1	91.92(12)	92.35(17)
O1-Mg-N2	114.29(11)	102.00(17)
O2-Mg-N2	109.35(11)	164.44(16)
O3-Mg-N1		138.85(17)
N1-Mg-N2	83.31(11)	79.74(18)

[a] Symmetry transformation used to generate equivalent atoms: [′] 1−x, 1−y, 1−z.

In the binuclear complex **2**, the two 2,6-*i*Pr$_2$C$_6$H$_3$-BIAN$^{-\bullet}$Mg units are bridged by a pinacolato dianion formed by dimerization of two benzophenone ketyl radical anions. The molecule is located on the crystallographic inversion center which lies in the middle of the C37–C37′ bond formed by dimerization of the ketyl radicals. This bond (1.605 Å) is significantly longer than a normal single C–C bond (1.54 Å), but is close to the length of comparable bonds in other pinacolato complexes,[9] except that in [{(SCN)$_2$Yb(thf)$_3$}$_2${μ-O$_2$C$_2$Ph$_4$}] (1.53 Å).[9e] The considerable length of this central C37–C37′ bond explains the easy homolytical splitting of **2** in solution leading to the biradical complex [(2,6-*i*Pr$_2$C$_6$H$_3$-bian)]$^{-\bullet}$[Mg(Ph$_2$CO)]$^{-\bullet}$ The geometrical arrangement of the coordinating ligand atoms N1, N2, O1, and O2 around each magnesium atom corresponds to that of a strongly distorted tetrahedron. The pinacolato bridge shows *trans* conformation. The oxidation of the 2,6-*i*Pr$_2$C$_6$H$_3$-BIAN^{2-} dianion in **1** to the 2,6-*i*Pr$_2$C$_6$H$_3$-BIAN$^{-\bullet}$ radical anion in **2** goes along with an elongation of the C1–C2 bond from 1.389 to 1.457 Å and a shortening of the N1–C1 and N2–C2 bonds from 1.401 to 1.324 Å and 1.378 to 1.331 Å, respectively. The Mg–N distances in **2** (2.107 and 2.079 Å) are longer than in **1** (1.995 and 2.004 Å),[8] thus reflecting the weaker interaction of the Mg cation with the radical anion than with the respective dianion. Due to the lengthening of the Mg–N bonds, the bite angle N1-Mg-N2 in **2** (83.3°) is smaller than that in the complex [(2,6-*i*Pr$_2$C$_6$H$_3$-bian)Mg(thf)$_2$]·(C$_6$H$_6$)$_{0.5}$ (90.7°).[8] Since no structural data concerning magnesium pinacolato complexes are deposited with CCDC, the Mg–O1 bond length (1.839 Å) in **2** is best compared with the Mg–O distances in magnesium alkoxy compounds for example, with the terminal Mg–O distance in the complex [Mg(μ-OCHPh$_2$)(OCHPh$_2$)(thf)]$_2$[13]

which shows a very close value (1.845 Å). The angle Mg-O1-C37 in **2** is 148.3°.

The X-ray structure analysis of $[(2,6\text{-}i\text{Pr}_2\text{C}_6\text{H}_3\text{-bian})^{-\bullet}\text{Mg}(\text{OC}_{14}\text{H}_9)(\text{thf})_2]$ (**3**) confirms that the reduction of 9(10*H*)-anthracenone with **1** leads to the formation of a 9-anthracenolato derivative. The coordination geometry of the magnesium atom is similar to that in **1**, showing the magnesium atom five coordinated in the center of a distorted trigonal bipyramid. Caused by the constraints imposed by the rigid chelating diimino ligand, N2 occupies an axial position, whereas N1 lies in the equatorial plane of the trigonal bipyramid. The second axial position is occupied by the THF O2 atom. As in complex **1** in which one of the two THF ligands fits into the pocket formed by two isopropyl groups each belonging to one of the two $i\text{Pr}_2\text{C}_6\text{H}_3\text{N}$ units of the BIAN ligand,[8] the 9-anthracenolato ligand in **3** takes up a comparable position (Figure 2b). The C–C and C–N bond lengths of the diimine unit of **3** (C1–C2 1.432 Å; N1–C1 1.334 Å; N2–C2 1.339 Å) are very close to those in complex **2** (1.457, 1.324 and 1.331 Å, respectively), thus proving the presence of the $2,6\text{-}i\text{Pr}_2\text{C}_6\text{H}_3\text{-BIAN}^{-\bullet}$ radical anion. Since no structure of a magnesium complex with terminal ArO ligands is documented as yet, the structural data of the magnesium 9-anthracenolato unit can not be compared with relevant fragments. However, the phenolic character of the 9-anthracenolato ligand may be deduced from the angle C37-O-Mg (164.1°), which is larger than the respective angle in **2** (148.3°), but approaches that in the thulium(III) complex $[\text{PhOTmI}_2(\text{dme})_2]$ (173.9°)[14] containing a terminal PhO ligand. Furthermore, the C43–C44 and C44–C45 bond lengths of 1.389 and 1.394 Å, respectively, confirm the aromatic character of the central ring. Due to the oxygen–arene conjugation, the bond length O1–C37 in **3** (1.303 Å) is much shorter than the respective bond in **2** (1.397 Å). On the other hand, the Mg–O1 bond in **3** (1.889 Å) is longer compared to the Mg–O1 bond in **2** (1.839 Å).

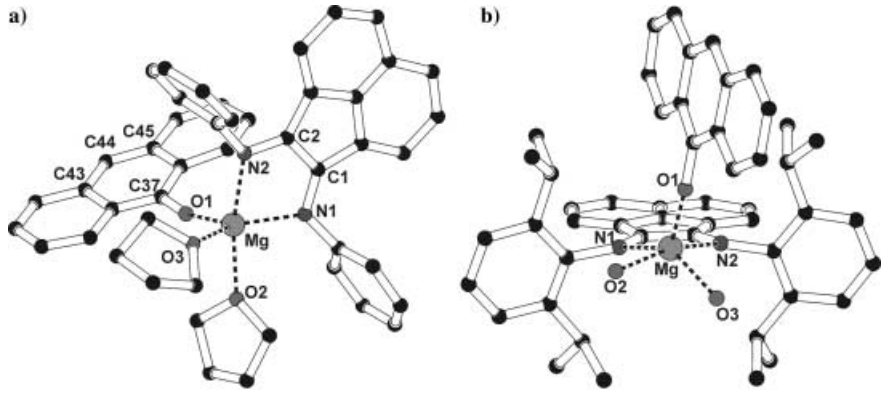

Figure 2. Molecular structure of **3**. a) Emphasis of the trigonal bipyramidal geometry of the Mg atom. The hydrogen atoms as well as the isopropyl groups at the N-phenyl substituents are omitted. b) Fitting of the anthryl-9-oxy ligand into the pocket formed by two isopropyl groups. The hydrogen atoms as well as the THF carbon atoms are omitted.

ESR and UV/Vis spectroscopic studies on solutions of 2 and 3: The radical-anionic character of the $2,6\text{-}i\text{Pr}_2\text{C}_6\text{H}_3\text{-BIAN}$ ligand in **2** is confirmed by the observation of a signal in the ESR spectrum of a toluene solution of the complex. This signal is only poorly resolved at room temperature, but shows a hyperfine structure due to the coupling of the unpaired electron with the ^{14}N and ^{1}H nuclei (multiplet, $A_N = 0.82$ mT, $2\times{}^{14}$N, $g = 2.0028$, Figure 3a) after cooling to 250 K. In the spectrum of the frozen solution at 130 K, the signal is further broadened, but shows a poorly resolved quintet structure. However, at this temperature, an additional signal appears consisting of four components (marked with asterisks in Figure 3b), the shape of which is typical for a biradical species. Based on the parameter of this signal ($D_{\|} = 32.5$ mT), the distance between the two unpaired electrons was calculated to be 5.5 Å, a value which is very close to the distance from the imino carbon atoms C1 and C2 to the carboxy atom C37 (5.58 and 5.61 Å, respectively) in solid **2**. Taking this fact into account, we conclude that in toluene solution a homolytic splitting of the benzpinacolato bridge takes place according to a transition of the dinuclear, *homo*-biradical **2** into the mononuclear, *hetero*-biradical magnesium benzophenone ketyl complex (Scheme 3). In solutions kept at ambient temperatures, the formation of such *hetero*-biradical species is hardly to prove by ESR measurements because of the broadening of the ESR signal under these conditions. However, the results of the UV/

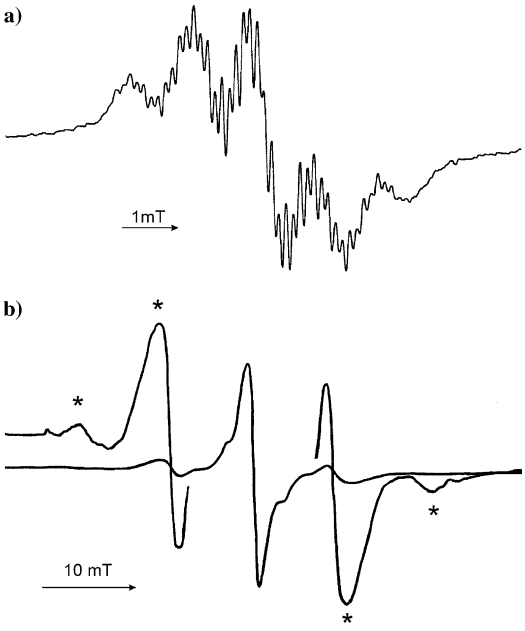

Figure 3. X-Band ESR spectra of **2** in toluene at 250 K (a) and 130 K (b). The asterisks indicate the components of the signal with respect to the biradical molecule $[(2,6\text{-}i\text{Pr}_2\text{C}_6\text{H}_3\text{-bian})^{-\bullet}\text{Mg}(\text{Ph}_2\text{CO})]^{-\bullet}$.

Vis spectra of toluene solutions of **2** recorded at room temperature indicate their existence.

The room temperature ESR spectrum of solutions of **3** in diethyl ether reveals a signal consisting of five components ($A_N = 0.83$ mT, $g = 2.0029$), indicating the coupling of the unpaired electron of the 2,6-iPr$_2$C$_6$H$_3$-BIAN radical anion with the two equal ^{14}N nuclei of this ligand. In contrast to the ESR spectra of **2**, the ESR spectra of ethereal solutions of **3** show no significant changes within the temperature range of 290 to 130 K, thus furnishing no evidence for the existence of biradical species.

The UV/Vis spectra of toluene solutions of **2** and **3** were recorded at room temperature in a pyrex glass cell (Figure 4). Especially the spectrum of **2** should allow to

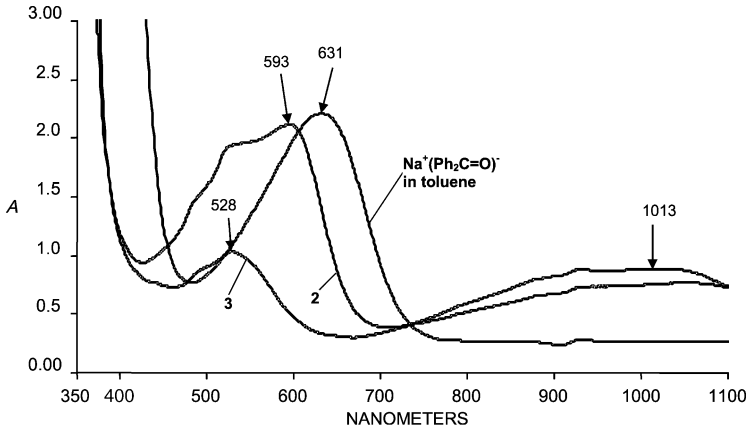

Figure 4. UV/Vis spectra in toluene of **2** (8.0×10^{-5} mol L^{-1}), **3**, and Na$^+$(Ph$_2$CO)$^-$.

decide if the hetero-biradical fragments, for which an absorption in the visible region is to be expected, are already formed at ambient temperature. The preparation of the toluene solution of **3** in a concentration similar to that of **2** (8.0×10^{-5} mol L^{-1}) needs special care (see Experimental Section) because of observable oxidation processes. Both, **2** and **3** show absorptions in the regions 450 to 600 and 750 to 1100 nm. Whereas the long-wave absorption is approximately of the same intensity for both complexes, the short-wave absorption of **3** is far less intense than that of **2**. Except the maximum at 593 nm in the spectrum of **2**, both short-wave absorptions show maxima at 445, 480 and 524 nm (**2**) or 443, 487, and 528 nm (**3**), respectively. One can suggest, that the band at 593 nm corresponds to the ketyl radical anion formed by homolytic splitting of the pinacolato bridge of complex **2**. For comparison and as a proof, we generated the benzophenone ketyl radical anion directly in the spectroscopic cell by reacting sodium with diphenylketone in toluene. The UV/Vis spectrum of this solution shows an absorption maximum at 631 nm. The relatively small long-wave shift compared to 593 nm, may be attributed to the different cations.

Conclusion

We could demonstrate that the recently prepared magnesium complex [(2,6-iPr$_2$C$_6$H$_3$-bian)Mg(thf)$_3$] (**1**)[8] containing the dianionic 1,2-bis[(2,6-diisopropyl-phenyl)imino]acenaphthene ligand serves well as reducing agent towards aromatic ketones. In contrast to the 1,3-dipolar cycloaddition of diphenylketone to dianionic 1,4-diaza-1,3-diene lanthanide or Group 4 metal complexes (Scheme 1), the reduction of Ph$_2$C=O with **1** affords the pinacol coupling product. The reduction of 9(10*H*)-anthracenone with **1** yields the aryloxy derivative as the result of the deprotonation of its phenolic tautomer 9-anthracenol. This anthracenyl-9-oxo derivative is the first example of a structurally characterized magnesium aryloxy complex containing a terminal OAr ligand. Further studies on the reactivity of [(2,6-iPr$_2$C$_6$H$_3$-bian)Mg(thf)$_3$] (**1**) towards organic substrates are in progress.

Experimental Section

General remarks: All manipulations were carried out under vacuum using Schlenk ampoules. THF, toluene, and diethyl ether were distilled from sodium/benzophenone prior to use. The melting points were estimated in sealed capillaries. 1,2-Bis[(2,6-diisopropylphenyl)imino]acenaphthene, (2,6-iPr$_2$C$_6$H$_3$-BIAN), was prepared according to the published procedure.[6a] The IR spectra were recorded on a Specord M80 spectrometer. The UV/Vis spectra were recorded on a Perkin-Elmer λ25 spectrometer using a pyrex glass cell ($15 \times 15 \times 30$ mm) which, in the case of **2**, was evacuated, filled with the toluene solution of **2**, and sealed under vacuum. In the case of **3**, the crystalline solid was placed into a pyrex glass cell which was connected with an ampoule containing toluene (Figure 5). The system was evacuated and sealed under vacuum. Subsequently toluene was condensed into the cell (slightly cooled by liquid nitrogen) causing partial dissolution of **3**. The toluene solution formed was decanted into the ampoule. The condensation/decantation procedure was repeated several times until the solution in the cell showed a transparency similar to the solution of **2**. The ESR spectra were recorded on a Bruker ER 200D-SRC spectrometer equipped with a low temperature controller ER 4111 VT and the signals were referred to the signal of diphenylpycrylhydrazil (DPPH, $g = 2.0037$).

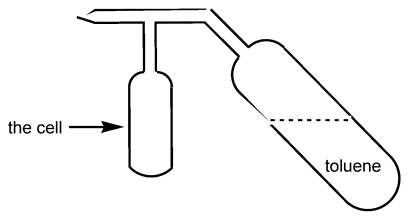

Figure 5. UV/Vis spectroscopic cell.

[(2,6-iPr$_2$C$_6$H$_3$-bian)Mg(thf)$_3$] (1): Magnesium shavings (2.4 g, 100 mmol) and CH_2I_2 (0.8 g, 2.98 mmol) were placed in a Schlenk-like ampoule (ca. 100 mL volume) equipped with a Teflon stopcock. After evacuation of the ampoule (10^{-1} Torr for ca. 1 min), THF (40 mL) was added by condensation and the mixture was stirred for 2 h. The [MgI$_2$(thf)$_n$] formed was decanted together with the solvent and the residual metal was washed three times with THF (40 mL). A suspension of 2,6-iPr$_2$C$_6$H$_3$-BIAN (0.5 g, 1.0 mmol) in THF (30 mL) was then added to the activated magnesium metal and the mixture was heated under reflux. After about 10 min of reflux, the reaction mixture had turned deep green. The solution was then cooled to ambient temperature and decanted from the

excess of magnesium. The THF solutions of **1** obtained were further used in situ for the reaction with benzophenone or 9(10*H*)-anthracenone.

[(2,6-*i*Pr$_2$C$_6$H$_3$-bian)Mg(thf)]$_2$[μ-O$_2$C$_2$Ph$_4$]·(C$_6$H$_6$)$_4$ (2): Benzophenone (0.18 g, 1.0 mmol) was added under stirring to the THF solution of **1** (obtained from 0.5 g (1.0 mmol) of 2,6-*i*Pr$_2$C$_6$H$_3$-BIAN in 30 mL THF). The solution instantly turned from deep green to red-violet. Evaporation of the solvent and crystallization of the crude product from benzene (20 mL) yielded **2** as red crystals (0.5 g, 54%). Concentration of the benzene solution left after the first crystallization to 10 mL afforded a second crop (0.21 g, 22%) of **2**. M.p. >116°C (decomp); IR (Nujol): $\tilde{\nu}$ = 1810 m, 1590 m, 1500 s, 1380 s, 1360 s, 1315 s, 1250 s, 1180 m, 1150 s, 1130 m, 1110 w, 1075 m, 1015 vs, 935 s, 865 s, 815 w, 795 m, 780 s, 755 vs, 745 s, 715 m, 705 m, 675 vs, 625 s, 545 w, 510 m, 455 w, 420 w cm^{-1}; elemental analysis calcd (%) for $C_{106}H_{116}Mg_2N_4O_4$·4 C_6H_6 (1871.08): C 83.45, H 7.54; found C 82.87, H 7.93; μ_{eff} = 2.57 BM.

[(2,6-*i*Pr$_2$C$_6$H$_3$-bian)·Mg(C$_{14}$H$_9$O)(thf)$_2$] (3): 9(10*H*)-Anthracenone (0.19 g, 1.0 mmol) was added under stirring to the solution of freshly prepared **1** (from 0.5 g (1.0 mmol) of 2,6-*i*Pr$_2$C$_6$H$_3$-BIAN in 30 mL THF). The mixture was stirred at 50°C for a few minutes until the mixture turned red. Evaporation of the solvent and crystallization of the remaining solid from Et_2O (25 mL) gave **3** as deep red crystals (0.45 g, 54%). M.p. >230°C; IR (Nujol): $\tilde{\nu}$ = 1565 w, 1530 m, 1315 w, 1245 m, 1220 w, 1180 s, 1110 s, 107 w, 1020 vs, 915 s, 875 s, 850 s, 815 s, 795 m, 765 s, 755 vs, 725 s, 675 w, 650 s, 615 s, 565 w, 505 w, 455 w, 420 w cm^{-1}; elemental analysis calcd (%) for $C_{58}H_{65}MgN_2O_3$ (862.43): C 80.77, H 7.60; found C 80.13, H 7.51; μ_{eff} = 1.87 BM.

Single crystal X-ray structure determination of 2 and 3: The crystal data and the details of the data collection are given in Table 1. The data for **2** and **3** were collected on a SMART CCD diffractometer (graphite-monochromated $Mo_{K\alpha}$ radiation, ω-scan technique, λ = 0.71073 Å). The structures were solved by direct methods and were refined on F^2 using all reflections with the SHELXL-97 program package.[15] In **2** two crystallographically independent isopropyl groups (C19–C21 and C22–C24) and two benzene solvent molecules (C61–C66 and C71–C76) are disordered about two positions. The C–C distances of the isopropyl groups and benzene molecules as well as the C-C-C angles of the latter were restrained to be equal. The respective occupancy factors were refined to 0.554(12)/0.446(12) (C19–C21), 0.574(16)/0.426(16) (C22–C24), 0.654(14)/0.346(14) (C61–C66), and 0.545(12)/0.455(12) (C71–C76). The carbon atoms of the disordered parts were refined isotropically, all other non-hydrogen atoms were refined anisotropically. The hydrogen atoms were placed in calculated positions and assigned to an isotropic displacement parameter of 0.08 Å^2. SADABS[16] was used to perform area-detector scaling and absorption corrections. The geometrical aspects of the structures were analysed by using the PLATON program.[17]

CCDC-211778 (**2**) and -211779 (**3**) contain the supplementary crystallographic data for this paper. These data can be obtained free of charge via www.ccdc.cam.ac.uk/conts/retrieving.html, or from the Cambridge Crystallographic Data Centre, 12 Union Road, Cambridge CB2 1EZ, UK; fax: (+44)1223–336033; or email: deposit@ccdc.cam.ac.uk.

Acknowledgement

This work was supported by the Russian Foundation for Basic Research (Grant No. 03-03-32246a), the Alexander von Humboldt Stiftung (I.L.F.), and the Fonds der Chemischen Industrie. The spectroscopic studies were carried out in the Analytical Center of the RAS (Grant RFBR No. 00-03-40116).

[1] a) R. van Asselt, E. E. C. G. Gielens, R. E. Rulke, C. J. Elsevier, *J. Chem. Soc. Chem. Commun.* **1993**, 1203–1205; b) R. van Asselt, K. Vrieze, C. J. Elsevier, *J. Organomet. Chem.* **1994**, *480*, 27–40; c) R. van Asselt, C. J. Elsevier, W. J. J. Smeets, A. L. Spek, R. Benedix, *Recl. Trav. Chim. Pays-Bas* **1994**, *113*, 88–98; d) R. van Asselt, C. J. Elsevier, *Organometallics* **1994**, *13*, 1972–1980; e) R. van Asselt, C. J. Elsevier, W. J. J. Smeets, A. L. Spek, *Inorg. Chem.* **1994**, *33*, 1521–1531; f) R. van Asselt, E. Rijnberg, C. J. Elsevier, *Organometallics* **1994**, *13*, 706–720; g) R. van Asselt, E. E. C. G. Gielens, R. E. Rulke, K. Vrieze, C. J. Elsevier, *J. Am. Chem. Soc.* **1994**, *116*, 977–985.

[2] M. W. van Laren, C. J. Elsevier, *Angew. Chem.* **1999**, *111*, 3926–3929; *Angew. Chem. Int. Ed.* **1999**, *38*, 3715–3717.

[3] R. van Belzen, H. Hoffmann, C. J. Elsevier, *Angew. Chem.* **1997**, *109*, 1833–1835; *Angew. Chem. Int. Ed. Engl.* **1997**, *36*, 1743–1745.

[4] E. Shirakawa, T. Hiyama, *J. Organomet. Chem.* **2002**, *653*, 114–121.

[5] a) D. Pappalardo, M. Mazzeo, S. Antinucci, C. Pellecchia, *Macromolecules* **2000**, *33*, 9483–9487; b) D. J. Tempel, L. K. Johnson, R. L. Huff, P. S. White, M. Brookhart, *J. Am. Chem. Soc.* **2000**, *122*, 6686–6700; c) D. P. Gates, S. A. Svejda, E. Onate, C. M. Killian, L. K. Johnson, P. S. White, M. Brookhart, *Macromolecules* **2000**, *33*, 2320–2334; d) S. A. Svejda, M. Brookhart, *Organometallics* **1999**, *18*, 65–74.

[6] a) A. A. Paulovicova, U. El-Ayaan, K. Shibayama, T. Morita, Y. Fukuda, *Eur. J. Inorg. Chem.* **2001**, 2641–2646; b) A. A. Paulovicova, U. El-Ayaan, K. Umezava, C. Vithana, Y. Ohashi, Y. Fukuda, *Inorg. Chim. Acta* **2002**, *339*, 209–214; c) D. S. Tromp, M. A. Duin, A. M. Kluwer, C. J. Elsevier, *Inorg. Chim. Acta* **2002**, *327*, 90–97; d) R. J. Maldanis, J. S. Wood, A. Chandrasekaran, M. D. Rausch, J. C. W. Chien, *J. Organomet. Chem.* **2002**, *645*, 158–167; e) M. Gasperini, F. Ragaini, S. Cenini, *Organometallics* **2002**, *21*, 2950–2957.

[7] I. L. Fedushkin, A. A. Skatova, V. A. Chudakova, G. K. Fukin, *Angew. Chem.* **2003**, 115, 3416–3420; *Angew. Chem. Int. Ed.* **2003**, *42*, 3294–3298.

[8] I. L. Fedushkin, A. A. Skatova, V. A. Chudakova, G. K. Fukin, S. Dechert, H. Schumann, *Eur. J. Inorg. Chem.* **2003**, 3336–3346.

[9] a) Z. Hou, T. Miyano, H. Yamazaki, Y. Wakatsuki, *J. Am. Chem. Soc.* **1995**, *117*, 4421–4422; b) Z. Hou, A. Fujita, H. Yamazaki, Y. Wakatsuki, *J. Am. Chem. Soc.* **1996**, *118*, 7843–7844; c) Z. Hou, A. Fujita, Y. Zhang, T. Miyano, H. Yamazaki, Y. Wakatsuki, *J. Am. Chem. Soc.* **1998**, *120*, 754–766; d) Z. Hou, T. Koizumi, M. Nishiura, Y. Wakatsuki, *Organometallics* **2001**, *20*, 3323–3328; e) G. B. Deacon, C. M. Forsyth, D. L. Wilkinson, *Chem. Eur. J.* **2001**, *7*, 1784–1795.

[10] R. Mahrwald, B. Ziemer, M. Ramm, *J. Prakt. Chem./Chem. Ztg.* **1996**, *338*, 583–587.

[11] J. Scholz, H. Görls, *Inorg. Chem.* **1996**, *35*, 4378–4382.

[12] J. Scholz, H. Görls, H. Schumann, R. Weimann, *Organometallics* **2001**, *20*, 4394–4402.

[13] C. A. Zechmann, T. J. Boyle, M. A. Rodriguez, R. A. Kemp, *Inorg. Chim. Acta* **2001**, *319*, 137–146.

[14] M. N. Bochkarev, A. A. Fagin, I. L. Fedushkin, T. V. Petrovskaya, W. J. Evans, M. A. Grici, J. W. Ziller, *Russ. Chem. Bull. Int. Ed.* **1999**, *48*, 1782–1786.

[15] G. M. Sheldrick, *SHELX-97 Program for Crystal Structure Determination*, Universität Göttingen (Germany), **1997**.

[16] G. M. Sheldrick, *SADABS Program for Empirical Absorption Correction of Area Detector Data*, Universität Göttingen (Germany), **1996**.

[17] A. L. Spek, *PLATON A Multipurpose Crystallographic Tool*, Utrecht University (The Netherlands), **2000**.

Received: June 13, 2003 [F5235]

